Available online at www.sciencedirect.com
SCIENCE DIRECT®
Journal of Nuclear Materials 351 (2006) 20–27
journal of nuclear materials
www.elsevier.com/locate/jnucmat

Two-band second moment model for transition metals and alloys

Graeme J. Ackland

Centre for Science at Extreme Conditions, School of Physics and Astronomy, The University of Edinburgh, James Clerk Maxwell Building, The King's Buildings, Mayfield Road, Edinburgh EH9 3JZ, UK

Abstract

A semi-empirical formalism based on the second moment tight-binding approach, considering two bands is presented for deriving interatomic potentials for magnetic d-band materials. It incorporates an empirical local exchange interaction, which accounts for magnetic effects without increasing the computing time required for force evaluation. The consequences of applying a two-band picture to transition metal alloys and transition metal impurities is examined, which combined with evidence from ab initio calculations leads to some surprisingly simplifying conclusions.

PACS: 61.80.Az; 71.20.Be; 61.82.Bg; 71.15.−m

1. Introduction

Semi-empirical models for metallic binding have had a long and successful history in computer modelling. The distinguishing features of models for metallic bonding are that they are short-ranged and non-pairwise. The first of these features arises from the strong screening of the nuclear charge by the mobile electrons, the second arises from the delocalisation of those electrons.

The most significant development in accounting for many-body effect came in the mid eighties with the implementation of 'embedded atom' potentials (EAM) [4] (based loosely on density functional theory [5]) and 'Finnis–Sinclair' potentials (FS) [6] (based on the tight-binding second moment approximation [7]). The two models have very similar computational requirements, and the names are often used interchangeably, however there are some distinctions which come to the fore when considering multicomponent alloys.

To highlight the differences, the energy according to the EAM is written:

$$U_{\mathrm{EAM}} = \sum_{ij} V_{IJ}(r_{ij}) + \sum_{i} F_I \left[\sum_{j} \phi_J(R_{ij}) \right], \qquad (1)$$

where i and j label atoms of element I and J respectively, V is a pairwise potential which depends on both species, F_I and ϕ_J are the embedding function and charge density which depend on one species only.

E-mail address: g.j.ackland@ed.ac.uk

0022-3115/$ - see front matter
doi:10.1016/j.jnucmat.2006.02.024

In slight contrast, the FS approach implies:

$$U_{\mathrm{FS}} = \sum_{ij} V_{IJ}(r_{ij}) + \sum_{i} F\left[\sum_{j} \phi_{IJ}(R_{ij})\right], \qquad (2)$$

where ϕ_{IJ} is the squared hopping integral between the atoms on-site i and site j and F is independent of the atomic species ($F(x) = \sqrt{x}$ in the second moment tight-binding approximation). In relating theses potential to tight-binding, there is a subtle issue of interpretation whether the many-body part is a *bond* or *band* energy [8] and extensions beyond second moment work explicitly with bonds [9]. While mindful of the distinction, for convenience the discussion here is presented in terms of bands projected onto atoms.

This subtle distinction becomes relevant for alloys: under EAM one requires no further refitting of the many-body function for each species, while the FS implies that a new ϕ_{IJ} function should be fitted for each pair of elements.

The success of ab initio methods in describing materials behaviour, and the possibility of using it directly to parameterise kinetic Monte Carlo simulations, may appear to negate the need for empirical potentials. However the lengthscales of correlated events involved in certain types of calculation – such as radiation damage cascades from fusion neutrons – are so large that empirical potentials still have a role to play.

Ab initio calculation has revealed a number of shortcomings in previous parameterisations of interatomic potentials for radiation damage application. In particular, when the original EAM parameterisation were done in the 1980s, the only information which affected the fit of the potential at short range came from isotropic compression: extrapolation of fits to empirical equations of state such as Murnaghan or Rose [1], or simple quantum electron gas calculations [2]. Recent total energy calculations reveal a picture in which isotropic compression of metals is resisted by many-body effects (such as electron kinetic energy), and that ions can approach one another rather more closely than had been predicted. A consequence of this is typically that interstitial formation energies are lower than in previous parameterisations had predicted, and the associated strain fields are smaller [3].

A philosophical issue arises at this stage. It is clear that such many body potentials cannot contain all the correct physics of the systems they are describing. What then should they aim to achieve?

In early work, it was attractive to show how the physical anomalies of pair potentials (zero Cauchy pressure, equivalence of vacancy formation and cohesive energy) can be eliminated with relatively little computational cost. In nuclear materials simulation however, the emphasis is less on physical elegance and more on practical application. In the multiscale modelling framework molecular dynamics modelling is simply an interpolation tool between exact ab initio and experimental results and the non-equilibrium behaviour of many-particle systems. Thus there is little justification for constraining the ability to precisely reproduce defect properties on the grounds of physical elegance. Consequently, recent parameterisations of 'many-body' (MB) models write the energy in the most general form:

$$U_{\mathrm{MB}} = \sum_{ij} V_{IJ}(r_{ij}) + \sum_{i} F_{I}\left[\sum_{j} \phi_{IJ}(R_{ij})\right], \qquad (3)$$

which for an N-component systems gives $N(N+1)$ functions available for fitting.

Most of the physical discussion motivating the potential centres on the form of the many-body term, the pairwise part representing 'everything else'. However, for high energy collisions and interstitials it is the pairwise part which tends to control behaviour.

It is possible to generate still more complex potentials with a similar computational cost to EAM. Examples include the MEAM [10], which incorporates angular effects in a way which uses only quantities already calculated in central-force molecular dynamics models, and the two-band model which describes the electronic state of each atom in an analytically solvable form [14].

One important system which is not easily described by these methods is iron. Although there have been a number of parameterizations for iron in a single phase, the essential physics leading to the stabilisation of the bcc phase is missing. Ab initio calculations show that without ferromagnetism, the fcc structure is favoured, and that the transition to the high pressure (hcp) or high temperature (fcc) phases is accompanied by a loss of ferromagnetism. Similarly, the atoms close to interstitial defects have a reduced magnetisation [12], which has the effect of making them more compressible.

In a recent paper [14], a simple two-band picture was derived for Cs to capture s–d electron transfer. This described the second moment tight-binding

energy in terms of a single parameter (the transfer of electrons between bands) at each site. Surprisingly, the parameterization proved transferrable across the transition metal series. Crucially for use in molecular dynamics, the minimum-energy value of this parameter can be evaluated at each atom independently and analytically, so the potential has the same computer requirement as EAM. Moreover, the energy is variational in this parameter, meaning that forces take a very simple form.

Here it is shown how a similar two-band picture within the second moment approximation can be developed to incorporate band ferromagnetism. In the simplest approximation, it give the surprising result that two-band effect can be captured in a standard many-body parameterisation, only the interpretation of the embedding function being changed.

2. Two d-band model-magnetism

2.1. Modified many-body term

In this section we show that incorporating band magnetism in the FS picture while ignoring the repulsion effect of enhanced Pauli exclusion gives rise to an embedded atom-type formalism with a non-monotonic embedding function.

In the second moment approximation to tight binding, the cohesive energy is proportional to the square root of the bandwidth, which can be approximated as a sum of pairwise potentials representing squared hopping integrals [6]. Assuming atomic charge neutrality, this argument can be extended to all band occupancies and shapes [15]. For simplicity, consider a rectangular d-band of full width W centred on E_0. The bond energy for a single spin band relative to the free atom is given by:

$$U^{\uparrow} = \int_{-W/2}^{E_f=\left(Z/N-\frac{1}{2}\right)W} NE/W \, \mathrm{d}E = \frac{Z^{\uparrow}}{N}\left(\frac{Z^{\uparrow}}{N}-1\right)NW/2, \tag{4}$$

where Z is the occupation of the band and uparrows denote 'spin up'.

To describe the ferromagnetic case, it is assumed that there are two independent d-bands corresponding to opposite spins, and that these can be projected onto an atom. In the atomic case Hund's rules lead to a spin of $S = 2$ for iron, and there is an energy U^x associated with transferring an electron to a lower spin state. In the solid, the simplest method is to set U^x to be proportional to the spin

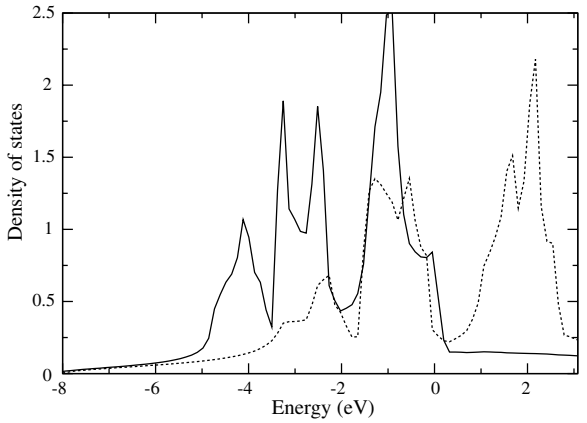

Fig. 1. BCC iron density of states for majority and minority spin bands from ab initio spin-dependent GGA pseudopotential calculations with 4913 k = points, adjusted so the ths Fermi energy lies at the zero of energy. The two-band model assumes that the bands have the same shape and width, but are displaced in energy relative to one another. Here it can be seen that this is the case.

with the coefficient of proportionality being an adjustable parameter, E_0

$$U^X = -E_0|Z^{\uparrow} - Z^{\downarrow}|. \tag{5}$$

Defining the spin, $S = |Z^{\uparrow} - Z^{\downarrow}|$ and noticing that with charge neutrality the total number of electrons at a site is conserved $T = (Z^{\uparrow} + Z^{\downarrow})$, we make the assumption that the bandwidth W is the same for each band (see Fig. 1). The two-band binding energy [14] for a d-band with capacity $N = 5$ on a site i is then:

$$\begin{aligned} U_i &= U_i^{\uparrow} + U_i^{\downarrow} + U_i^X \\ &= +\frac{W_i}{4N}(T^2 + S_i^2) - TW_i/2 - E_0 S_i. \end{aligned} \tag{6}$$

This equation gives us the optimal value for the magnetisation of a given atom of $S_i = 2NE_0/W_i$, and the many-body energy of an atom with $T = 6$, $N = 5$ (suppressing the i label) as:

$$\begin{aligned} U &= -6W/5 - 5E_0^2/W \quad E_0/W_i \leqslant 0.4, \\ &= -2W/5 - 4E_0 \quad E_0/W_i \geqslant 0.4, \end{aligned} \tag{7}$$

which introduces the constraint that there is a maximum value for S. For a material with T d-electrons (where $T > 5$). transfer of electrons between the spin bands becomes advantageous for $W > 10E_0/(10 - T)$. For smaller W the spin $\uparrow$ band is full and the energy is simply proportional to the bandwidth of the $\downarrow$ band as in the Finnis–Sinclair model.

Within the second moment model, the bandwidth W is given by the square root of the sum of the squares of the hopping integrals [7]. This sum can be represented by a pairwise potential and is the same for each band.

$$W_i = \sqrt{\sum_j \phi(r_{ij})}. \tag{8}$$

Interatomic potentials also include the effect of the ions and non-valence electrons: this is usually represented by a simple pairwise potential. This gives us the final functional form for incorporating magnetism in the ferromagnetic regime within the Finnis–Sinclair formalism:

$$E = \sum_j \left[\sum_i V(r_{ij}) - \sqrt{\rho_j} - B/\sqrt{\rho_j} H(2W - 5E_0) - 4E_0 H(5E_0 - 2W) \right], \tag{9}$$

where H is the Heaviside step function, B is a constant, $\rho_j = \sum_i \phi(r_{ij})$, V and ϕ are empirically fitted pairwise potentials, and the zero of energy is shifted to correspond to the *non-magnetic* atom.

Note that this form does not explicitly include S, and that it has the form of the embedded atom model with an embedding function $F_I(x) = \sqrt{x}(1 - B/x)$. In particular, the local magnetisation means that the embedding function now depends on the type of atom through the amount of the particular band projected onto it.

Although this model incorporates magnetism, and provides a way to calculate the magnetic moment at each site, it is possible to use it without actually calculating S – the implementation with an additional many-body repulsive term is similar to the many-body potential method of Mendelev et al. [11]. In terms of forces and energetics, it will perform in a similar way. In particular, there is no first order magnetic transition.

The anomaly with this model is that the linear expression for U^X leads to a non-zero magnetisation at all densities (although this becomes vanishingly small at high densities). If instead of Eq. (5) we use a Stoner-type quadratic term $U^X = I_0 S^2$ this changes the Eq. (6) such that the spin state flips from fully magnetised to fully demagnetised at $W_i = 4NI_0$.

Neither of these behaviours is quite correct, and a better treatment involves making the pairwise term spin-dependent, which is the subject of the following section.

2.2. Incorporating Pauli repulsion

Pauli repulsion arises from electron eigenstates being orthogonal. While its nature on a single atom is complex, its interatomic effects can be modelled as a pairwise effect of repulsion between electrons of similar spins. The secondary effect of magnetisation is that there are more electrons in one band than another, more same-spin electron pairs to repel one another, and so the repulsion between those bands is enhanced. Using the Stonor-type $U^X = I_0 S^2$, the many-body energy on an atom becomes

$$\begin{aligned} U &= U^{\uparrow} + U^{\downarrow} + U^X \\ &= +\frac{W}{4N}(T^2 + S^2) - TW/2 + I_0 S^2. \end{aligned} \tag{10}$$

This shows that a high magnetisation changes the energy in two ways, firstly by effectively widening the bands and secondly via I_0.

We now consider the pairwise repulsive part of the potential. Conceptually, this contains two effects, the standard paramagnetic repulsion which represents the screened Coulomb repulsion of the ions and the core–core repulsion, and an additional S_i dependent term arising from Pauli repulsion between like-spin electrons.[1] Writing this in a separable form:

$$V(r_{ij}) = V_0(r_{ij}) + (S_i + S_j) V_m(r_{ij}). \tag{11}$$

The total energy on the ith atom is then

$$U_{\text{tot}} = \sum_i \left[-TW_i/2 + (S_i^2 + T^2) W_i/4N + S_i I + \frac{1}{2}\sum_j V_0(r_{ij}) + S_i \sum_j V_m(r_{ij}) \right]. \tag{12}$$

The key to this step how we 'assign' the Pauli energy to each atom. If we choose to do it such that the energy assigned to each atom i depends only on

[1] Note there are issues about antiferromagnetism here. An AFM state with $S_i + S_j = 0$ would have a lower repulsive energy. In the tight-binding picture this would be compensated by a much reduced hopping integral and hence lower W. If we insist on $S_i > 0$ then we suppress these solutions and can model ferromagnetic or diamagnetic iron. Also, as with DFT-GGS/LDA the spin is Ising-like.

the value of S_i at that atom, this allows us to minimise $U_{\rm tot}$ with respect to $\{S_i\}$ at each site *independently* which gives us:

$$S_i = \frac{-2N}{W_i}\left[I + \sum V_m(r_{ij})\right]. \tag{13}$$

Values of S_i are bounded by 0 and $2N - T$. Thus, we can solve analytically for S, and the computational cost of the calculation becomes equivalent to a standard EAM.

The energy depends variationally on the values of S_i: $\partial U/\partial S_i = 0$. This allows application of the Hellmann–Feynman theorem in the force calculation to eliminate terms involving changes in S_i.

Thus the complexity of the forces is also just like EAM

$$F_i = \sum_j \frac{1}{2}\frac{\mathrm{d}V_0}{\mathrm{d}r_{ij}} + S_i\frac{\mathrm{d}V_m}{\mathrm{d}r_{ij}}\hat{\mathbf{r}}_{ij} \tag{14}$$

$$+\left(\frac{S_i^2+T^2}{4N} - \frac{T}{2}\right)\sum_j \frac{\mathrm{d}\phi}{\mathrm{d}r_{ij}}\hat{\mathbf{r}}_{ij} \tag{15}$$

$$+\sum_j \left(\frac{S_j^2+T^2}{4N} - \frac{T}{2}\right)\frac{\mathrm{d}\phi}{\mathrm{d}r_{ij}}\hat{\mathbf{r}}_{ij}. \tag{16}$$

To make a potential, one needs to fit the pairwise functions $V(r_{ij})$ and $\phi(r_{ij})$ and the parameter I_0. This model can be generalised from the Finnis–Sinclair form to the EAM form by using a parameterised embedding function rather than the square root.

3. Two-band model for alloys

3.1. Transition metal alloys

An alternative use of a two d-band model occurs when an alloy of two d-metals is formed. The difficulty with one band on each atom is that charge transfer between sites becomes non-local and minimising energy becomes non-analytic [14]. It is possible to use a fictitious dynamics for the charge transfer, in the same spirit as Car-Parinello, but this would introduce a large number of additional equations of motion.

The convenient solution, implicit in Eq. (3), is to assume that a similar d-band can be projected onto both sites, shifted for charge neutrality. This would allow us to use the MB approach. Here we investigate whether such an assumption can be justified. Fig. 2 shows a density of states for a MoV alloy. The notable feature is that the alloy bands are narrower than the pure metal bands, suggesting that $2\phi_{\rm AB}(r_{ij}) < \phi_{\rm AA}(r_{ij}) + \phi_{\rm BB}(r_{ij})$.

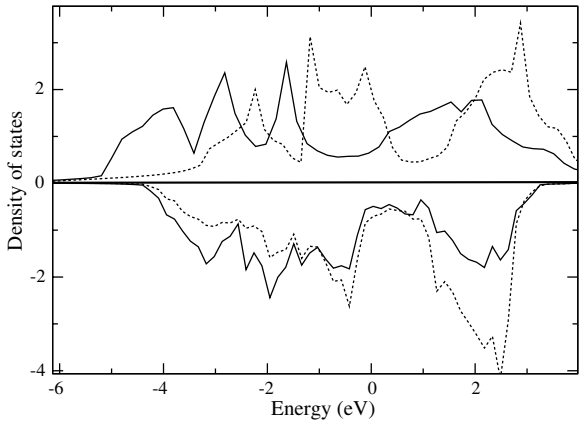

Fig. 2. Density of states from ab initio GGA pseudopotential calculations with 4913k = points, adjusted so that the Fermi energy lies at the zero of energy. Upper bands: pure V (dots) and Mo (solid) at their equilibrium structure (bcc, 3.006 Å and 3.184 Å, respectively). Lower bands (plotted upside down for ease of comparison): MoV alloy in CsCl structure (lattice parameter 3.086 Å), with density of states projected onto the two atoms according to the integrated electron density within 1.5 Å of the nucleus. Further 16-atom supercell calculations for single substitutional Mo in V and Cu in Fe show similarly undifferentiated bands, although when semi-core p-electrons are included in the valance band this method show near-perfect localisation.

Furthermore, calculations of the projected density of individual electron states onto individual atoms for isolated Mo and V and for Cu in Fe shows that there are no localised d-states – the band structure is projected fairly evenly onto each species.

3.2. p-band impurities – C, P

The presence of non-transition metal impurities in steels is of major interest for a wide range of applications. The combination of p- and d-based materials makes for a complicated band structure and the picture of simply adding electrons to a rigid band is no longer tenable. Fig. 3 shows the ab initio calculated density of states for Fe_3C cementite, compared with the density of states calculated for the identical arrangement of Fe atoms with the carbons removed.

The first striking feature is that the occupied carbon bands can be readily distinguished in Fe_3C. Unoccupied carbon p-bands lie well above the Fermi energy, meeting the requirement for charge neutrality which underlies the idea of and band energy determined from a local density of states [15]. This suggests that, in the FS picture at least,

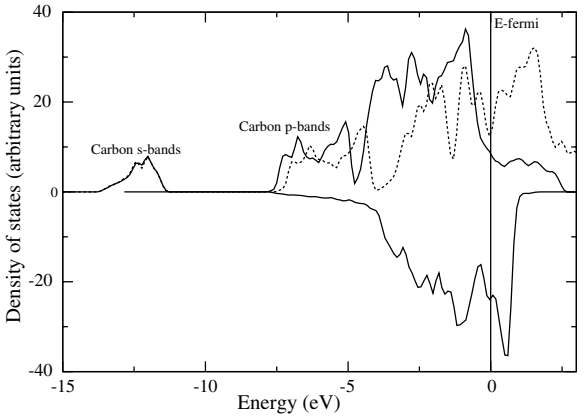

Fig. 3. Density of states from ab initio GGA pseudopotential calculation with 1000k = points. Upper bands: Fe_3C cementite with atomic positions and unit cell are fully relaxed ($a = 5.069$ Å, $b = 6.744$ Å, $c = 4.514$ Å). Lower bands: unit cell containing Fe in the same locations as cementite, but no carbon, this gives a non-ferromagnetic ground state.

the hopping integral between bands can be ignored. Furthermore, the carbon bands lie far below the Fermi energy. This suggests that they will not contribute to the metallic bonding and cannot be treated in the same way as the d-electrons. This means that to a first approximation one can set $\phi_{FeC}(r) = 0$, and treat the iron–carbon interaction purely as a pair potential.

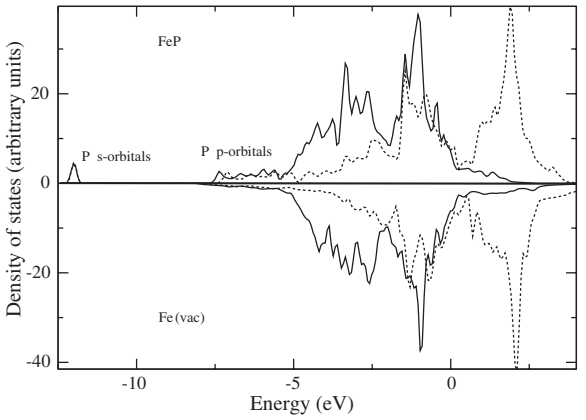

Fig. 4. Density of states from ab initio GGA pseudopotential calculations with 729k = points, adjusted so that the Fermi energy lies at the zero of energy. Upper bands: supercell of 15 iron atoms with a substitutional P impurity, relaxed to its equilibrium volume (186 $Å^3$) with ions relaxed and magnetic moment 35.3μ_B. Lower bands:supercell of 15 iron atoms with a vacancy, relaxed to its equilibrium volume (183.7 $Å^3$) with ions relaxed and magnetic moment 36.4μ_B. Note that the two densities of state are extremely similar, the main effect of the P being the addition of two low lying s-states and some additional p-states and the low energy end of the d-band.

Similar unhybridised carbon states have been seen for isolated defects: the one occasion when the bonding of the dissolved carbon changes qualitatively being the formation of a covalent bond in a C dimer located in a Fe vacancy [13].

A similar same situation applies to embedding a phosphorus atom in iron. The phosphorus s-electrons play no part in the bonding, and the p-states lie below the d-band (Fig. 4).

4. Multiple elements without refitting

Finnis–Sinclair type models have had reasonable success in modelling interatomic alloys of transition metals, here the extension of the theory is straightforward. If accurate results for radiation damage are required, then some refitting is necessary. For alloys with low concentrations of impurities, such as reactor steels, a more straightforward approach may be appropriate. With the simple two-band iron model above, we can assume that the main effect of small concentrations of local impurities is not to change the shape of the projected band structure, but to change the number of electrons in the band. As before, the MB energy can be separated into contributions from each atom:

$$U = \sum_i U_i^{\uparrow} + U_i^{\downarrow} + U_i^{XC}$$
$$= +\frac{W}{4N}(T_i^2 + S_i^2) - T_i W/2 - E_{i0}S_i, \qquad (17)$$

following the procedure adopted for Cs [14] an approximate potential for an embedded transition metal impurity can be made using the same parameters as for iron with lengths scaled by the Fermi vector ($T^{-1/3}$) and energies by $T^{1/2}$. The separation of the pair potential into the form:

$$V_{IJ}(r_{ij}) = V_I(r_{ij}) + V_J(r_{ij}) \qquad (18)$$

implies that the screening for the impurity is due to *the iron charge density*. Hence such a pairwise potential would not be transferrable to environments of high concentration of the impurity atom. It is already well known that potentials fitted to give a good description of the dilute environment show poor transferrability across the phase diagram [16,17].

5. Potentials for molecular dynamics – or vice versa

The concept of designing interatomic potentials is typically to start with a full quantum mechanical

treatment of the electrons, and then via a series of approximations arrive at a form suitable for use in molecular dynamics. Hence EAM is formulated as a extreme localised form of the density functional theory, while Finnis–Sinclair is a simplified tight binding. It is unclear to what extent the correctness of the original physics is retained – certainly in applications empirical refitting is used to 'fold back' all the missing physics in an approximate way.

The ultimate test of the usefulness of a potential is its transferrability – does it work in environments different from where it was fitted? If it is transferrable, it is quite acceptable for a potential to include arbitrarily introduced terms to compensate for the uncontrolled approximations made from the full quantum mechanical treatment.

Hence an alternate view of potentials is to *start* with the needs of molecular dynamics and ask what functional forms are possible. The constraints are that we require short-ranged interactions based on atomic positions only. The potential may then use any information available from the molecular dynamics to reproduce the forces correctly. In fact, much information is available in a real molecular dynamics calculation which might be useful in formulating the potential.

For simplicity, we assume the calculation does not explicitly evaluate three-body terms – this involves an additional calculational overhead and there are no such terms in the full many-body quantum mechanical Hamiltonian. The following quantities can be evaluated:

(a) Functions of separations at each atom (EAM's 'electron density' or FS's 'sum of squared hopping integrals).
(b) Functions of other rotationally invariant quantities at each atom (as in MEAM) [10].
(c) On-site parameters with respect to which the energy can be minimised *locally* and *analytically* (as in the two-band model [14]).
(d) The mean electron density, and the free electron Fermi energy.

5.1. Evaluating and using the Fermi energy

Almost all quantum treatments of metals require calculation of the Fermi energy. In the Finnis–Sinclair approach it is the fixing of the Fermi level combined with the condition of charge neutrality which allows the method to work for other than half-filled bands [15]. Further, it has been known since Hume–Rothery that Fermi surface effects lies at the heart of the structural properties of metallic alloys.

In principle, a short-ranged potential cannot incorporate such effects, because the Fermi energy depends on delocalised electrons: an extremely long-range effect. However, in setting up a molecular dynamics simulation, all the information needed to calculate the Fermi level is often included. Most radiation damage calculations entail a constant volume ensemble simulation of a bulk material with a few defects: the mean electron density is known and constant throughout, and the Fermi level can therefore be established. In surface calculations there appears to be a problem, however even here the molecular dynamics uses boundary conditions (periodic slab geometry, fixed layer, etc.) which are intended to represent contact with a bulk of fixed density. Again, the Fermi Energy for this can readily be established. In constant pressure simulations, it may appear that the Fermi energy should vary, yet even this is unclear – in standard Parrinello–Rahman dynamics an expansion of the region of interest is accompanied by and expansion of all periodic-image supercells. In the case of a phase transition, this is reasonable and the Fermi energy can track the density, however in other cases the local expansion would actually cause a compression in the surrounding region, preserving the Fermi energy at its bulk value. Hence either treatment of the Fermi level has equally good physical justification as the Parrinello–Rahman scheme itself.

Thus there should be no objection to using the Fermi Energy as part of the formulation of a potential, since its value can readily be determined at the outset of a molecular dynamics calculation.

One anomaly this removes is the series of phase transitions under pressure exhibited by empirical potentials: e.g. even the 0 K ground state of the Lennard–Jones potential switches between fcc and hcp as a function of pressure [21], though no real material does this. Other close-packed metal potentials behave similarly. The reason for this is that phase stability depends on the long-range part of the potential – beyond second neighbours at equilibrium. Under compression various shells of neighbours come into the range of the potential, increasing or decreasing the energy of the two phases.

The resolution to this problem has long been known. Thirty-five years ago Heine and Weaire [18] showed that within pseudopotential theory phase stability for simple metals the energy could be

calculated as a volume term independent of atomic positions, plus a pair potential with asymptotic form:

$$V(R) \propto \frac{\cos(2k_F R + \phi)}{(2k_F R)^3}. \quad (19)$$

The key point here is that $k_F R$ is close to constant for isotropic compression. Hence this term will not contribute to the change in relative phase stability under pressure. The r^{-3} form can be made usable in molecular dynamics if the long-range pairwise part is damped with an exponential [19]: this corresponds to a finite electron temperature and does not significantly affect the forces. The same fictitious-electron-temperature approximation is used routinely in ab initio calculations where it is known as 'Fermi smearing'.

Recently, potentials which attempt to measure the density ρ_i with local sampling have appeared [20]: the most effective local sampling measure seems to be a sum of a Gaussian potential. These allow the pair potential to depend explicitly on the electron density and take the form:

$$U = \sum_{ij} V_I(r_{ij}, \rho_i) + \sum_i F_I\left[\sum_j \phi_{IJ}(R_{ij})\right]. \quad (20)$$

However, as discussed above, for practical molecular dynamics such short range approximations to find the Fermi energy (and their associated calculational cost) are unnecessary.

6. Conclusions

In this paper, we have laid out how the ideas underlying the two-band model, already applied to caesium [14], can be extended to magnetic elements such as iron and its alloys. By way of ab initio simulation we have shown how the site-projected density of states, which forms the conceptual framework behind Finnis–Sinclair type potentials, suggest particular approaches to different systems. In particular, if magnetism is introduced without affecting the pairwise potential, an EAM-type model is recovered – the onsite magnetisation need only be calculated if different Pauli repulsion for majority and minority bands is assumed. Similarly, for sp-bonded impurities C and P in iron, we find valence states well below the Fermi energy and little effect on the d-bands. This suggests that these impurities can be sensibly treated with pair potentials + unmodified many-body iron potential, unless they get close enough to bond to one another.

Accurate parameterisations are not presented here, rather the paper points the way to developing future interatomic potentials and provides some post facto justification for previous studies.

References

[1] J.H. Rose, J.R. Smith, F. Guinea, J. Ferrante, Phys. Rev. B 29 (1984) 2963.
[2] G.J. Ackland, R. Thetford, Philos. Mag. A 56 (1987) 15.
[3] S. Han, L.A. Zepeda-Ruiz, G.J. Ackland, R. Car, D.J. Srolovitz, Phys. Rev. B 66 (22) (2002) 220101.
[4] M.S. Daw, M.I. Baskes, Phys. Rev. B 29 (1984) 6443.
[5] P. Hohenberg, W. Kohn, L.J. Sham, Phys. Rev. 136 (1964) B864.
[6] M.W. Finnis, J.E. Sinclair, Philos. Mag. A 50 (1984) 45.
[7] F. Ducastelle, J. Phys. Paris 31 (1970) 1055.
[8] D.G. Pettifor, in: D.G. Pettifor, A.H. Cottrell (Eds.), Electron Theory in Alloy Design, IoM, London, 1992, p. 81.
[9] D.G. Pettifor, Phys. Rev. Lett. 63 (1989) 2480.
[10] M.I. Baskes, Phys. Rev. B 46 (1992) 2727.
[11] M.I. Mendelev, S.W. Han, D.J. Srolovitz, G.J. Ackland, D.Y. Sun, M. Asta, Philos. Mag. A 83 (2003) 3977.
[12] C. Domain, C.S. Becquart, Phys. Rev. B 65 (2002) 024103.
[13] C. Domain, C.S. Becquart, J. Foct, Phys. Rev. B 69 (2004) 144112.
[14] S.K. Reed, G.J. Ackland, Phys. Rev. B 67 (2003) 174108.
[15] G.J. Ackland, V. Vitek, M.W. Finnis, J. Phys. F 18 (1988) L153.
[16] E.M. Lopasso, M. Caro, A. Caro, P.E.A. Turchi, Phys. Rev. B 68 (2003) 214205.
[17] G.J. Ackland, D.J. Bacon, A.F. Calder, T. Harry, Philos. Mag. A 75 (1997) 713.
[18] V. Heine, D. Weaire, Solid State Phys. 24 (1970) 249.
[19] D.G. Pettifor, M.A. Ward, Solid State Commun. 49 (1984) 291.
[20] M.W. Finnis, A.B. Walker, P. Gumbsch, J. Phys.: Condens. Matter 10 (1998) 7983.
[21] A.N. Jackson, A.D. Bruce, G.J. Ackland, Phys. Rev. E 65 (3) (2002) 036710.